



Original article

Astaxanthin Ameliorates high-fat diet-induced cardiac damage and fibrosis by upregulating and activating SIRT1

Abdullah S. Shatoor^{a,*}, Suliman Al Humayed^b^a Department of Medicine, Cardiology Section, College of Medicine, King Khalid University (KKU), Abha, Saudi Arabia^b Department of Internal Medicine, College of Medicine, King Khalid University (KKU), Abha, Saudi Arabia

ARTICLE INFO

Article history:

Received 18 May 2021

Revised 25 July 2021

Accepted 27 July 2021

Available online 30 July 2021

Keyword:

Astaxanthin
Inflammation
Fibrosis
Heart
High fat diet
Oxidative stress
Rats
SIRT1

ABSTRACT

This study evaluated the protective effect of astaxanthin (ASX) against high-fat diet (HFD)-induced cardiac damage and fibrosis in rats and examined if the mechanism of protection involves modulating SIRT1. Rats were divided into 5 groups (n = 10/group) as: 1) control: fed normal diet (3.82 kcal/g), 2) control + ASX (200 mg/kg/orally), 3) HFD: fed HFD (4.7 kcal/g), 4) HFD + ASX (200 mg/kg/orally), and 5) HFD + ASX + EX-527 (1 mg/kg/i.p) (a selective SIRT1 inhibitor). All treatments were conducted for 14 weeks. Administration of ASX reduced cardiomyocyte damage, inhibited inflammatory cell infiltration, preserved cardiac fibers structure, prevented collagen deposition and protein levels of TGF- β 1 in the left ventricles (LVs) of HFD-fed rats. In the LVs of both the control and HFD-fed rat, ASX significantly reduced levels of reactive oxygen species (ROS), tumor necrosis factor- α (TNF- α), interleukin-6 (IL-6), and p-smad2/3 (Lys19) but increased the levels of glutathione (GSH), catalase, and manganese superoxide dismutase (MnSOD). Concomitantly, it increased the nuclear activity of Nrf2 and reduced that of NF- κ B p65. Furthermore, administration of ASX to both the control and HFD-fed rats increased total and nuclear levels of SIRT1, stimulated the nuclear activity of SIRT1, and reduced the acetylation of Nrf2, NF- κ B p65, and Smad3. All these cardiac beneficial effects of ASX in the HFD-fed rats were abolished by co-administration of EX-527. In conclusion, ASX stimulates antioxidants and inhibits markers of inflammation under basal and HFD conditions. The mechanism of protection involves, at least, activation SIRT1 signaling.

© 2021 The Authors. Published by Elsevier B.V. on behalf of King Saud University. This is an open access article under the CC BY-NC-ND license (<http://creativecommons.org/licenses/by-nc-nd/4.0/>).

1. Introduction

Cardiac remodeling is the leading mechanism of developing cardiac dysfunction and heart failure (HF) with subsequent increase in morbidity and mortality (Webber et al., 2020). At the same time, obesity is a modifiable risk factor that is associated with metabolic-cardiovascular disorders and HF among children, young, and adults (Carbone et al., 2019; Cercato and Fonseca, 2019). In this regard, it was shown that obesity can damage the heart and induces cardiac hypertrophy, fibrosis, and hemodynamic

alterations by promoting cardiac oxidative stress and inflammation, mainly by inducing hyperglycemia, hyperlipidemia, systemic and cardiac insulin resistance (IR), and cardiac lipotoxicity (Ebong et al., 2014; Nakamura and Sadoshima, 2020; Gutiérrez-Cuevas et al., 2021). Weight loss, calorie restriction, and pharmacological drugs (i.e. glucose-lowering, hypolipidemic, and insulin-sensitizing drugs) remain the available options to manage HF in obese individuals (Dunlay et al., 2019; Jindal et al., 2013). Accordingly, natural antioxidants and/or anti-inflammatory agents represent novel therapies to alleviate cardiac damage and remodeling in obese patients and animals (Aimo et al., 2020; Geng et al., 2019).

On the other hand, current investigations are focusing on the emerging roles of sirtuins (SIRT) proteins, and particularly SIRT1 in the modulating diverse cardiovascular disorders (CVDs) in humans (Elibol and Kilic, 2018; Matsushima and Sadoshima, 2015). In the cardiomyocytes, SIRT1, an NAD⁺-dependent class III histone deacetylases, stimulates cell survival and antioxidant capacity but inhibits oxidative stress, inflammation, and fibrosis by deacetylating several transcription factors including the nuclear factor erythroid 2-related factor 2 (Nrf2) and Forkhead Box O

* Corresponding author.

E-mail addresses: asshalghamdi@yahoo.com, ashalghamdi@kku.edu.sa (A.S. Shatoor).

Peer review under responsibility of King Saud University.



Production and hosting by Elsevier

(FOXO), two masters antioxidant transcription factor, the nuclear factor-kappa beta (NF- κ B), a master inflammatory inducer, and the Smad3 fibrotic transcription factor (Chong et al., 2012; Matsushima and Sadoshima, 2015). SIRT1-deficient mice suffered from severe developmental heart defects, dilated cardiomyopathy, and a reduced survival rate (Matsushima and Sadoshima, 2015). However, reduced cardiac levels and activities of SIRT1 were reported in high-fat diet (HFD)-induced obese animal models, as well as in animals with other CVDs and HF (i.e. diabetic cardiomyopathy, ischemia/reperfusion (I/R) injury, myocardial infarction (MI), and Dahl salt-sensitive rats), and were correlated with the degree of the cardiac damage, oxidative stress, inflammation, fibrosis, and apoptosis (Chong et al., 2012; Matsushima and Sadoshima, 2015; Favero et al., 2020; Fry et al., 2016; Huang et al., 2014). Besides, SIRT1 polymorphism was associated with an increased risk of CVDs in the Iranian population (Mohtavinejad et al., 2015). Therefore, findings drugs that target SIRT1 will provide an interesting therapy to treat obesity-induced cardiac remodeling and HF.

Astaxanthin (ASX) (C₄₀H₅₂O₄) is a carotenoid that is isolated from deeply colored microorganism's marine species (i.e. microalgae, crayfish, salmon, and shrimp) and is known for its powerful antioxidant, immunomodulatory, anti-inflammatory, and anti-fibrotic properties (Landon et al., 2020). The cardioprotective effects of ASX have been reported in humans and animals (Fassett and Coombes, 2011; 2012; Kato et al., 2020). In this review, 3-months supplementation of ASX to patients with HF improved the LV ejection fraction (LVEF), extended their 6-min walking distance, and decreased markers of oxidative stress (Kato et al., 2020). Also, ASX prevented cardiac muscle damage and preserved left ventricular LV function after heavy exercise, ischemia/reperfusion, and myocardial infarction (MI)-induced cardiac injury by suppressing oxidative stress and inflammation (Adluri et al., 2013; Aoi et al., 2003; Gross and Lockwood, 2004; 2005). In addition, ASX improved cardiac contractility and attenuated cardiac inflammation in BALB/c Mice (Nakao et al., 2010). Interestingly, in a recent study, Zhang et al. (Zhang et al., 2017) have shown that ASX can protect against pressure overload-induced cardiac dysfunction and myocardial fibrosis, partially by activating SIRT1.

Up-to-date, the protective effect of ASX against obesity or HFD-induced cardiac damage and remodeling was never studied before. Therefore, we assumed that chronic supplementation of ASX could attenuate HFD-induced LV oxidative stress, inflammation, and interstitial fibrosis in rats by activating SIRT1 signaling and subsequent deacetylation of Nrf2, NF- κ B p65, and Smad3, whereas co-administration of EX-527, a selective SIRT1 inhibitor prevents this.

2. Materials and methods

2.1. Animals

Adult Wistar male rats (150 \pm 15 g/7 weeks old) were supplied and kept in the animal facility department at King Khalid University (KKU) in Abha, Kingdom of Saudi Arabia. All rats were always lived under fixed ambient conditions (23 \pm 1 °C, 61–62% humidity, and 12/12 h light/dark cycle) and always had free access to their designed diet and drinking water. All the procedures and protocols conducted in this study were approved by the institutional animal care unit which follows the guidelines of the US National Institutes of Health (NIH publication No. 85-23, revised 1996).

2.2. Animal diets

Both normal diet (cat D12450B) and HFD (cat D12451) for rats were used in this study and have been previously used by others to induced obesity-mediated cardiomyopathy (Wang et al., 2018). The total energy of the normal diet was 3.82 kcal/g in which 10%, 20%, and 70% were derived from fat, protein, and carbohydrates, respectively. The total energy obtained from the HFD was 4.7 kcal/g in which 40%, 20%, and 40% were derived from fat, protein, and carbohydrates, respectively. The ingredients of both diets are shown in Table 1.

2.3. Experimental design

After 1 week adaptation period, the rats were randomly classified into 5 groups (n = 10/each) as 1) control rats: fed normal diet and orally administered the vehicle (1% DMSO dimethyl sulfoxide (DMSO) (cat 472301, Sigma Sigma-Aldrich, MO, USA) diluted in phosphate buffer saline (PBS/pH = 7.4); 2) control + ASX-treated rats: fed normal diet and orally administered ASX (prepared in 1% DMSO/PBS) (cat SML0982, Sigma Sigma-Aldrich, MO, USA), at a final dose of 200 mg/kg; 3) HFD-fed rats: fed HFD and orally administered 1% DMSO solution; 4) HFD + ASX-treated rats: fed HFD and orally treated with ASX (200 mg/kg), and 5) HFD + ASX + EX-527-treated rats: fed HFD and co-treated with ASX (200 mg/kg/orally) and EX-527 (a selective SIRT1 inhibitor) (1 mg/kg/i.p) (cat E7034, Sigma Sigma-Aldrich, MO, USA). ASX and DMSO were administered orally by gavage and all treatments were conducted for 14 weeks. During our preliminary data, a period between 10 and 16 weeks was shown to induce cardiac injury and fibrosis in rats after chronic feeding with this procided HFD.

2.4. Dose selection

The dose of ASX and EX-527 was based on the study of Zhang et al. (Zhang et al., 2017) who have shown the ability of ASX at this dose to prevent cardiac injury and fibrosis and preserve cardiac function in a mouse model of pressure overload-induced cardiac damage which can be blocked by such i.p. dose of EX-527.

Table 1
Composition of the standard (STD) and high-fat diet (HFD).

| Classic description | Ingredients | Normal diet g/diet | HFD g/diet |
|------------------------|-----------------------------------|--------------------|------------|
| Protein | Cystine, L | 3 g | 3 |
| Protein | Casein, Lactic, 30 Mesh | 200 | 200 |
| Carbohydrate | Starch.corn | 315 | 72 |
| Carbohydrate | Lodex 10 | 35 | 100 |
| Carbohydrate | Sucrose | 354 | 176 |
| Fiber | Solka Flocc, FCC200 | 50 | 50 |
| Fat | Soybean Oil, USP | 25 | 25 |
| Fat | Lard | 20 | 177 |
| Mineral | S10026B | 50 | 50 |
| Vitamin | Choline bitartrate | 2 | 2 |
| Vitamin | V10001C | 1 | 1 |
| Dye | Yellow FD&C #5, Alum. Lake 35–42% | 0.05 | 0.05 |
| Protein | | 20% | 20% |
| Carbohydrate | | 70% | 40% |
| Fat | | 10% | 40% |
| Total Calorie (kcal/g) | | 3.82 | 4.7 |

2.5. Serum and tissue collection

By the end of week 14, 12 h-fasted rats of all groups were anesthetized by an i.m. dose of ketamine/xylazine solution (80/12 mg/kg). Blood samples (2 ml) were collected directly from the heart into either EDTA-containing or plain tubes and then centrifuged at 1200 \times g for 1 min at room temperature to collect the plasma or serum samples, which both were preserved at -20°C . All rats were then authenticated by the cervical dislocation and their hearts were rapidly collected on ice. The LVs were identified, separated, and cut into smaller parts. Some parts were directly fixed in a 10% buffered formalin solution whereas the other parts were snap-frozen in liquid nitrogen and stored at -80°C for further use.

2.6. Preparation of tissue homogenates and cytoplasmic/nuclear fractions

To prepare total cell homogenates for the biochemical analysis and western blotting, parts of LVs were homogenized in 9 volumes of either PBS (pH = 7.4) or radioimmunoprecipitation (RIPA) buffer (plus protease inhibitor), respectively, and the supernatants were collected after centrifugation at 12,000 \times g for 10 min at 4°C . The cytoplasmic/nuclear fractions of all LVs were prepared using a commercially available isolation kit following the manufacturer's instructions (cat 113474, Abcam, Cambridge, UK). The purities of both the cytoplasmic and nuclear fractions were confirmed by western blotting by detecting the presence or absence of the cytoplasmic and nuclear markers, α tubulin and lamin A, respectively, using their specific primary antibodies (cat sc-5286, Santa Cruz Biotechnology, CA, USA and cat 86846, Cell Signaling Technology, MA, USA, respectively).

2.7. Biochemical analysis in the serum and LV homogenates

All kits used for this part were rats' specific. Plasma levels of fasting glucose and insulin levels were measured using special ELISA kits as per the manufacturers' instructions (cat 81693; Crystal Chem, IL, USA, and cat MBS2700141, MyBioSource, CA, USA respectively). Serum levels of Troponin-I (Tn-I) and creatinine kinase-MB (CKMB) were determined by ELISA (cat MBS727624, cat MBS2515061 My BioSource, CA, USA, respectively). LV levels of ROS were measured by using an assay kit (cat STA-347, Cell Biolabs, CA, USA). LV levels of major antioxidants anti-inflammatory cytokines including manganese superoxide dismutase (MnSOD), total glutathione GSH, catalase, interleukin-6 (IL-6), and tumor necrosis alpha (TNF- α) were measured using ELISA kits (cat MBS729914, cat MBS046356, cat MBS726781, cat MBS175908, and cat MBS175904; MyBioSource, CA, the USA respectively). All measurements were conducted as per each kit instruction. The activation of Nrf2 and NF- κ B in the nuclear fractions was measured using ELISA kits (cat 50296 and cat AM 40596, Active Motif, Tokyo, Japan). The activity of SIRT1 in the nuclear fraction was measured using a fluorometric kit (cat Ab156065, Abcam, Cambridge, UK).

2.8. Western blotting

This has been done following our established procedures (Shatoor and Al Humayed, 2020). Protein concentrations in the total, cytoplasmic, and nuclear fractions were measured by BCA protein assay kit (cat 71285-M, Sigma Sigma-Aldrich, MO, USA). Total, cytoplasmic, and nuclear proteins were prepared in the SDS loading buffer at a final concentration of 2 $\mu\text{g}/\text{kg}$, boiled for 5 min, and separated (40 $\mu\text{g}/\mu\text{l}$) at various ratios of SDS PAGE (8–15%). The membranes were then blocked with 5% skimmed milk prepared in 1X TBST (tris-buffered saline, 0.1% Tween 20), electrically transferred using the *trans*-blot SD semi-dry transfer

cell (BioRad, USA) (20 mV for 20 min), and then washed with 1X TBST buffer for 3 times at room temperature each of 10 min. The membranes were then incubated, individually, with the primary antibodies against SIRT1 (cat sc-74465, 120 kDa, 1:1000), β -actin (cat sc-8432, 45 kDa, 1:1000), tubulin α (cat sc-5286, 55 kDa, 1:1000), lamin A (cat sc-293162, 1:1000), TGF- β 1 (cat sc-130348, 25 kDa, 1:1000), (Santa Cruze biotechnology, CA, USA), p-Smad 3 (Ser^{423/425}) (cat 9520, 52 kDa, 1:500), COL1A1 (cat 39952, 220 kDa, 1:1000) (Cell signaling Technology, MA USA), and acetyl-smad2/smud3 (Lys¹⁹) (cat PA5-76015, 52 kDa, 1:1500), Acetyl NF- κ B (Lys³¹⁰) (cat PA5-17264, 65 kDa, 1:500) (Thermo-Fisher Scientific Inc., NJ, USA), and Acetyl Nrf2 (Lys⁵⁹⁹) (cat STJ9230, 61 kDa, 1:500, St John's Laboratory Ltd, London, UK) for 2 h at room temperature with continuous shaking. The membranes were washed again with the 1X TBST buffer as above and then incubated with the 2nd HRP-conjugated antibody for another 2 h at room temperature. After a final wash, the interaction between the antibodies (Bands) was detected by incubating each membrane with the ECL chemiluminescence reagents (cat 32109, T Thermo-Fisher Scientific Inc., NJ, USA USA) and bands were scanned using a special scanner (model C-Di Git, LI-COR, NE, USA). The expressions of all nuclear proteins were normalized with lamin A were as the expression of the cytoplasmic and total proteins were normalized with tubulin α and t β -actin, respectively.

2.9. Histological evaluation

Formalin-Fixed tissues were directly rehydrated in increasing concentration of ethanol (70–100%) and then cleared with xylene. All tissues were then embedded in paraffin and cut into 3–5 μm sections. The tissues were routinely stained b either hematoxylin and eosin (H&E) or Masson trichrome stain for normal histological evaluation or detection of fibrosis, respectively. All slides were examined by a blind pathologist who is unaware of the experimental groups under a light microscope.

2.10. Statistical analysis

All data were analyzed using version 8 of the GraphPad Prism statistical software. The Kolmogorov-Smirnov test was used for normality testing. The comparison and degree of significance between different groups were analyzed by one-way ANOVA followed by Tukey's *t*-test. The values were considered significantly varied to $P < 0.05$.

3. Results

3.1. Effect on metabolic parameters

Final body weights (BW), heart weights, heart/BW ratio, fasting glucose, insulin, and FFAs levels were significantly increased in the HFD-fed group as compared to the control rats (Table 2). However, administration of ASX didn't affect any of these parameters in both the control and HFD-fed rat, except it significantly reduced heart weights and heart/BW ratio, only in HFD-fed rats (Table 2). On the other hand, with no significant variation in final body weights, fasting glucose, insulin, and FFAs levels, heart weights and heart/BW ratio were significantly increased in HFD + ASX + EX-527 as compared to HFD + ASX-fed rats, values which were not significantly different as compared to HFD-fed rats (Table 2).

3.2. Effect on circulatory levels of cardiac markers

On the other hand, no significant variations in the serum levels of CK-MB and Troponin-1 were seen between the control and

Table 2

Final body, heart weights, and circulatory levels of free fatty acids (FFAs) creatinine kinase-MB (CK-MB) and Troponin-I (Tn-I) in all groups of rats.

| HFD + ASX + EX-527 | HFD + ASX | HFD | Control + ASX | Control | Parameter |
|----------------------------|---------------------------|---------------------------|---------------|-------------|--|
| 531 ± 27 ^{ab} | 519 ± 29 ^{ab} | 529 ± 35 ^{ab} | 429 ± 31 | 437 ± 28 | Final body weight (g) |
| 1.59 ± 0.17 ^{abd} | 1.28 ± 0.19 ^c | 1.65 ± 0.12 ^{ab} | 1.18 ± 0.21 | 1.21 ± 0.18 | Heart weights (g) |
| 311 ± 0.19 ^{ab} | 2.56 ± 0.27 ^c | 3.23 ± 0.23 ^{ab} | 2.78 ± 0.25 | 2.71 ± 0.21 | Heart/BW ratio (×10⁻³) |
| 178.4 ± 11.5 ^{ab} | 184 ± 8.6 ^{ab} | 187 ± 12.5 ^{ab} | 110 ± 10.1 | 105 ± 9.4 | Fasting plasma glucose (mg/dl) |
| 5.2 ± 0.67 ^{ab} | 5.3 ± 0.61 ^{ab} | 5.6 ± 0.55 ^{ab} | 3.3 ± 0.54 | 3.1 ± 0.48 | Fasting plasma insulin (ng/ml) |
| 848 ± 38.2 ^{ab} | 867 ± 41.5 ^{ab} | 882 ± 51.1 ^{ab} | 328 ± 26.3 | 318 ± 22.5 | Serum FFAs (μM) |
| 456 ± 27.9 ^{abd} | 256 ± 31.1 ^{abc} | 428 ± 24.9 ^{ab} | 219 ± 22.1 | 212 ± 17.5 | Serum CK-MB (pg/ml) |
| 385 ± 18.6 ^{abd} | 178 ± 16.9 ^{abc} | 391 ± 24.1 ^{ab} | 153 ± 13.1 | 143 ± 11.5 | Serum Tn-I (pg/ml) |

Data were analyzed for n = 10 samples/group and were significantly different $p < 0.05$. ^a: vs. the control rats; ^b: vs. the control + ASX-treated rats; ^c: vs. HFD-fed rats, ^d: vs. HFD + ASX-treated rats. EX-527: a selective SIRT1 inhibitor.

control + ASX-treated rats (Table 2). Levels of both markers were significantly increased in HFD-fed rats as compared to control rats but were significantly decreased in the serum of HFD + ASX-treated rats (Table 2). On the other hand, serum levels of both CK-MB and Troponin-1 were significantly increased in the serum of HFD + ASX + EX-527 when compared to HFD + ASX-treated rats, levels which were not significantly different as compared to HFD-fed rats (Table 2).

3.3. Effect on cardiac structure

Normal LVs structures were observed in both the control and control + ASX-treated rats (Fig. 1A and B). On the other hand, LVs of HFD-fed rats showed increased damaged muscle fiber, karyolytic nuclei, hypertrophied muscles, and increased inflammatory cell infiltration in their LVs (Fig. 1C and D). Almost normal architectures with few cardiomyocyte damage and the presence of some inflammatory cell infiltration were observed in the LVs of HFD + ASX-treated rats (Fig. 1F and G). However, similar pathological changes like those observed in the hearts of HFD-fed rats were also observed in the LVs of HFD + ASX + EX-527 (Fig. 1H).

3.4. Effect on collagen deposition and TGF-β1/Smad3 signaling

Similar amounts of collagen with no significant changes in the total protein levels of TGF-β1 and COL1A1 were seen between the LVs of the control and control + ASX-treated rats. However, nuclear protein levels of p-Smd3 (Ser^{423/425}) and acetyl Samd3 (Lys¹⁹) were significantly decreased in control + ASX-treated rats as compared to control rats (Fig. 2A-H). Higher amount of collagen fibers with significantly higher total protein levels of TGF-β1 and COL1A1, as well significantly higher nuclear protein levels of p-Smd3 (Ser^{423/425}) and acetyl Samd3 (Lys¹⁹) were seen in the LVs of HFD-fed rats as compared to control rats which were then significantly reduced in HFD + ASX-treated rats (Fig. 2A-H). On the other hand, levels of all these fibrotic markers with increased collagen deposition were seen in the LVs of HFD + ASX + EX-527 as compared to HFD + ASX-treated rats (Fig. 2A-H). Of the note, protein levels of TGF-β1, COL1A1, p-Smd3 (Ser^{423/425}), and acetyl Samd3 (Lys¹⁹) were not significantly varied between the HFD-fed rats and HFD + ASX + EX-527 (Fig. 2A-H).

3.5. Effect on markers of oxidative stress and inflammatory cytokines

Levels of ROS, TNF-α, and IL-6 were significantly increased whereas levels of GSH, catalase, and MnSOD were significantly reduced in the LVs of HFD-fed rats as compared to control rats (Fig. 3A-F). However, levels of ROS, TNF-α, and IL-6 were significantly decreased whereas levels of GSH, catalase, and MnSOD were significantly increased in the LVs of both the control + ASX and HFD + ASX-treated rats as compared to either the control or

HFD-fed rats, respectively (Fig. 3A-F). However, Levels of ROS, TNF-α, and IL-6 were significantly increased whereas levels of GSH, catalase, and MnSOD were significantly reduced in the LVs of HFD + ASX + EX-527-treated rats as compared to HFD + ASX-treated rats, all of which were not significantly different as compared to HFD-fed rats (Fig. 3A-F).

3.6. Effect on SIRT1 levels and activity and the acetylation of Nrf2 and NF-κB p65

Total protein levels, nuclear protein level, and nuclear activity of SIRT1 were significantly decreased in the LVs of HFD-fed rats as compared to control rats (Fig. 4A, C, & D). Concomitantly, the nuclear activity of Nrf2 was significantly reduced and the nuclear activity of NF-κB p65 was significantly enhanced with increased acetylated levels of Nrf2 and NF-κB p65 in the LVs of HFD-fed rats as compared to control rats (Fig. 4B&D). Total activity and total and nuclear protein levels of SIRT1, as well the nuclear activities of Nrf2 and NF-κB p65 were significantly increased the acetylated protein levels of Nrf2 and NF-κB p65 were significantly reduced in the LVs of HFD + ASX-treated rats as compared to HFD-fed rats (Fig. 4A-D). All these effects were reversed in HFD + ASX + EX-527 as compared to HFD + ASX-treated rats where the activities/expressions of all these markers were not significantly different as compared to HFD-fed rats (Fig. 4A-D).

4. Discussion

The salient findings of the present study provide the first evidence in the literature that the cardioprotective effect of ASX against HFD -induced cardiac damage and remodeling involve antioxidant, anti-inflammatory, and anti-fibrotic effects mediated, at least, by upregulation and activation of SIRT1 and subsequent deacetylation of several targets including Nrf2, NF-κB p65, and Smad3.

The process of cardiac damage during obesity is a very complicated process that involves several mechanisms. Oxidative stress and inflammation induced by the altered cardiac substrate preference (i.e. FFAs), impaired mitochondria function, cardiac steatosis, altered adipokines profile, cardiac IR, as a result of dysfunctional adipose tissue, systemic and cardiac IR, and hyperglycemia, are the major events leading to cardiac damage and remodeling during obesity (Dludla et al., 2017; Nakamura and Sadoshima, 2020). In the failing heart, damaged mitochondria, over-activated NADPH oxidase in the cardiac myocytes, endothelial cells, and neutrophils, and low levels of the endogenous antioxidant are the major sources of ROS (Tsutsui et al., 2011). However, adipose tissue-derived inflammatory cytokines and those derived locally from the infiltrating monocytes and macrophages, in response to cardiac damage and oxidative stress, trigger cardiac inflammation. Accordingly, ROS can damage the cardiomyocytes and promotes hyper-

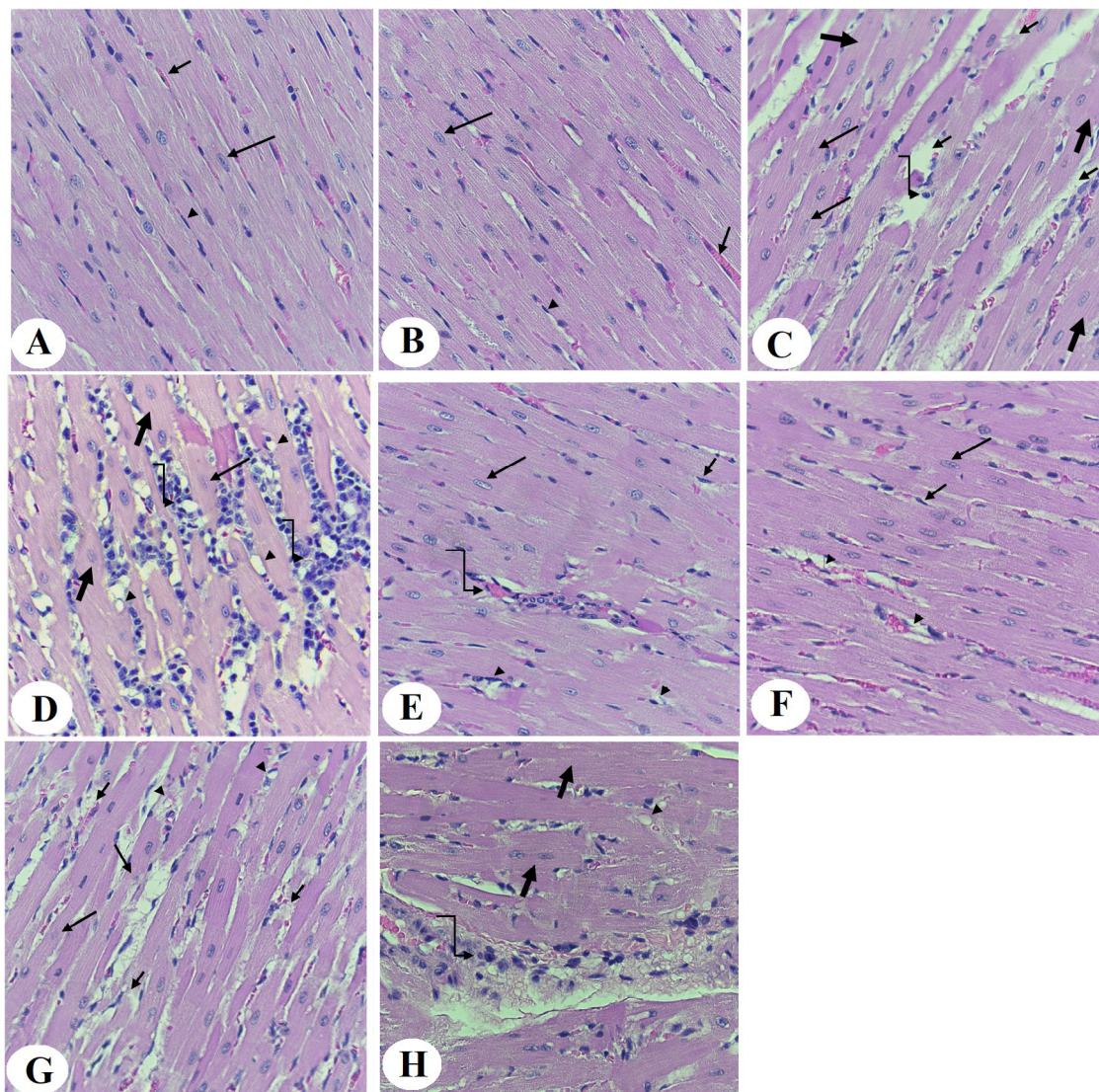


Fig. 1. Histological photomicrographs of the left ventricles (LVs) of all groups of rats. Haematoxylin and eosin (H & E) stain (400 X). *A & B:* were taken from control and control + ASX-treated rats and show normal architecture with normally sized striated cardiomyocytes that contain central intact nuclei (long arrow) and peripheral endothelial cells (arrowheads), and blood vessels (short arrows). *C & D:* were taken from LVs of HFD-fed rats and showed abnormal cardiomyocyte structure with increased fiber damage (short arrow), nuclear fading (karyolysis) (long arrow), vacuolization (arrowhead), hypertrophied muscle fibers (thick arrow), an increase in inflammatory cell infiltration (curved arrow). *E & F:* were taken from LVs of HFD + ASX-treated rats and showed much improvement in the cardiomyocyte structure with intact normally sized muscle fibers that have normal nuclei (long arrow) and endothelial cells (short arrow). However, some muscle fiber damage (arrowhead) and inflammatory infiltration (curved arrow) are still seen. *G & H:* were taken from HFD + ASX + EX-527-treated rats and showed a similar picture to that seen in HFD-fed rats where cardiomyocytes damage (short arrow), karyolitic nuclei (long arrow), vacuolization (arrowhead) hypertrophied muscle fibers (thick arrow), and increased inflammatory cells infiltration (curved arrow) were abundant.

trophy, inflammation, apoptosis by activating numerous damaging pathways (i.e. MAPKs, ASK1, JNK, TGF- β 1/Smad2/3, ANGII, and NF- κ B) (De Marchi et al., 2013; Gutiérrez-Cuevas et al., 2021; Tsutsui et al., 2011). Besides, ROS disturbs cardiac contractility by targeting Ca^{2+} handling pumps such as the RyR and SERCA proteins (Nakamura and Sadoshima, 2020). On the other hand, TNF- α and IL-6 act in a vicious cycle to stimulate the generation of ROS from the cardiac cells and promotes cardiac fibrosis by activating the TGF- β 1/Smad2/3 axis (Suthahar et al., 2017). Also, both cytokines induce cardiac hypertrophy by interacting and activating nuclear factors of activated T cells (NFAT) (Liu et al., 2012).

In the same line of the above-mentioned evidence, HFD-fed rats showed a significant increase in the weight of their hearts, fasting hyperglycemia, hyperinsulinemia, and higher levels of ROS and inflammatory cytokines in their hearts. Besides, their LVs showed severe damage with increased collagen fiber deposi-

tion. In addition, they showed increased activation of NF- κ B p65, reduced expression of antioxidants (MnSOD, GPx, and GSH), a reduction in the nuclear activities of Nrf2, and hyperactivation of the TGF β 1/Smad3 axis. These findings support many other previous studies (Favero et al., 2020; Geng et al., 2019; Huang et al., 2014). On the other hand, ASX was able to attenuate all these effects in HFD-fed rats without modulating circulatory levels of glucose and insulin. Besides, ASX also failed to altered glucose and insulin levels, as well as the expression of TGF β 1 in the hearts of the control rats but significantly stimulated the antioxidant levels and Nrf2 activity and suppressed the activation of NF- κ B, levels of ROS, MDA, TNF- α , IL-6, and the phosphorylation of Smad3 in the hearts of the control rats. Based on this, we have concluded that the cardiac protective effect of ASX entails antioxidants, anti-inflammatory, and anti-fibrotic effects mediated by activation of Nrf2 and suppression of NF- κ B p65 and Smad3.

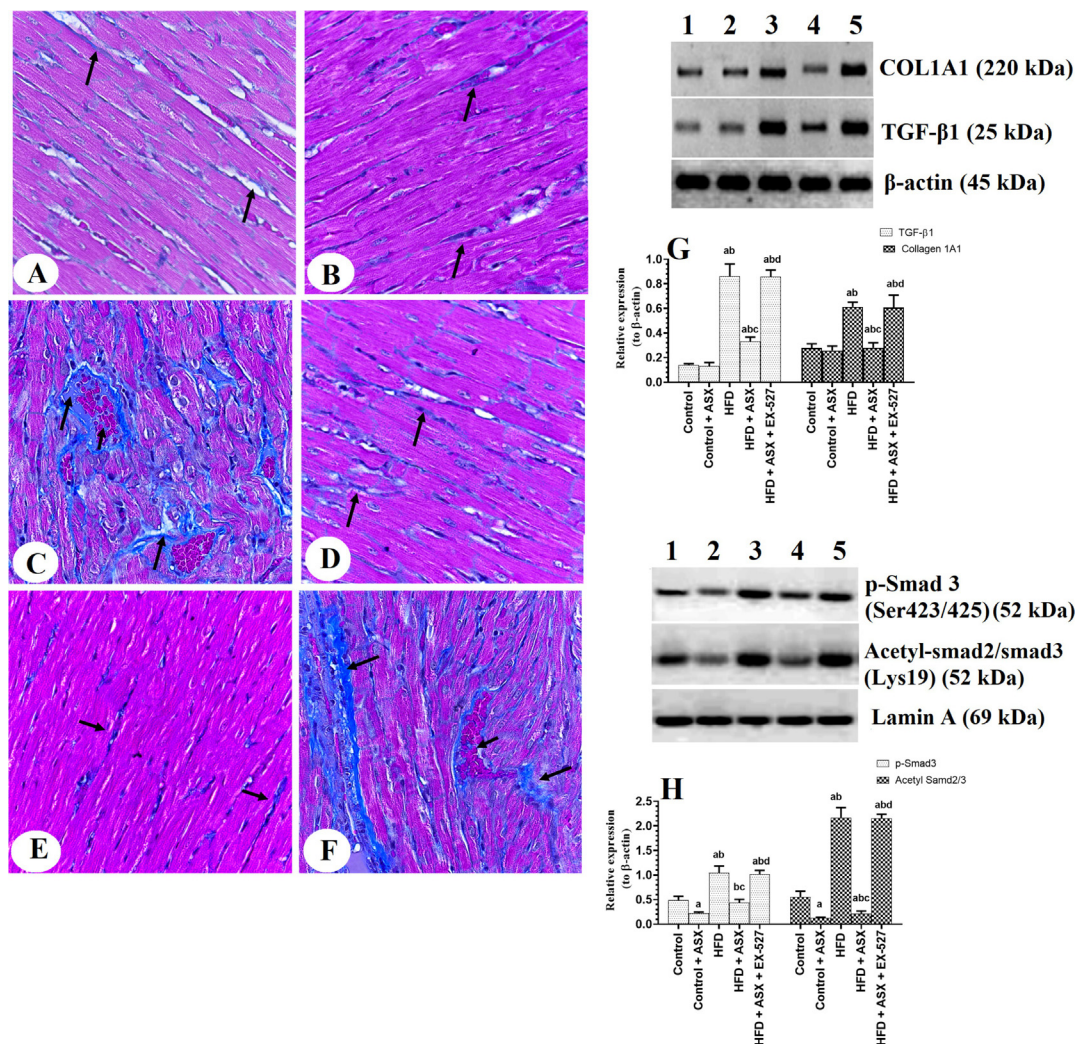


Fig. 2. Collagen deposition (A–F) and protein levels of some fibrotic genes in the left ventricles (LVs) of all groups of rats. A–F: Masson trichrome stain (400X). The black arrow in A–F indicates the number of collagen fibers deposited in each LV sample. A & B: were taken from LVs of control and control + ASX-treated rats and showed few collagen fibers. C: was taken from the LV of an HFD-fed rat and showed increased collagen deposition and interstitial fibrosis. D and E: were taken from LVs of HFD + ASX-treated rats and showed a significant reduction in the amount of collagen fiber as compared to HFD-fed rats. F: was taken from LV of HFD + ASX + EX-527-treated rats and showed increased collagen deposition. In G–H: Data were analyzed for $n = 6$ samples/group and were significantly different $p < 0.05$. ^a: vs. the control rats; ^b: vs. the control + ASX-treated rats; ^c: vs. HFD-fed rats; ^d: vs. HFD + ASX-treated rats. EX-527: a selective SIRT1 inhibitor.

Indeed, activation of Nrf2 and ablation of IL-6, TNF- α , or NF- κ B completely protected against diabetic and HFD-induced cardiomyopathy and remodeling (Dludla et al., 2017; Nakamura and Sadoshima, 2020). In different animal models, the protective effect of ASX was attributed to scavenging ROS, upregulating antioxidants and Nrf2, improving mitochondria function, and inhibiting NF- κ B and inflammatory cytokines production (Kavitha et al., 2013; Kim and Kim, 2018; Landon et al., 2020; Priyadarshini and Aggarwal, 2018; Zhu et al., 2018). Also, ASX prevented hepatic and pulmonary fibrosis in several animal models by silencing the TGF- β 1/Smad3 signaling and the concomitant suppression of NF- κ B, ROS, TNF α , and IL-6 (Shen et al., 2014; Wakabayashi et al., 2015; Zhang et al., 2015).

Supporting our data, many authors have also shown no effect of ASX on glucose and insulin homeostasis in diabetic animals (Chan et al., 2012; Landon et al., 2020). On the other hand, other studies contradict our data and have shown hypoglycaemic and insulin-sensitizing effects of ASX in diabetic and other animal models (Arunkumar et al., 2012; Bhuvaneshwari and Anuradha, 2012; Hussein et al., 2007; Preuss et al., 2011). Such variation between our data and those studies could be attributed to the variation in

the animal model and the dose of ASX used, animal species (mice vs. rats), source of ASX (natural vs. synthetic), treatment period, and the method of ASX administration. Also, ASX improved cardiac contractility under basal conditions and cardiac injury in rodents by mitigating ROS generation, oxidative stress, and inflammation, and upregulating antioxidants (Aoi et al., 2003; Fassett and Coombes, 2011; 2012; Kato et al., 2020). In both the control, obese, and HF patients, ASX increased cardiac contractility, stimulated total antioxidant capacity, and mitigated serum and urinary levels of markers of oxidative stress and lipid peroxidation (Choi et al., 2011; Kato et al., 2020; Park et al., 2010). In the same line, ASX antagonized oxidative stress, improved mitochondria membrane potential, and increased contractility index in BALB/c mice (Nakao et al., 2010). Moreover, ASX reduced infarction size and reversed LV structure and function in mice, rats, dogs, and rabbits by upregulating antioxidants and reducing the generation of ROS, macrophage infiltration, inflammatory cytokine production, and activation of TGF- β 1/Smad2/3 signaling (Adluri et al., 2013; Fassett and Coombes, 2011; 2012; Gross and Lockwood, 2004; 2005; Lockwood and Gross, 2005; Pan et al., 2020). Also, ASX improved cardiac structure and function and prevented coronary

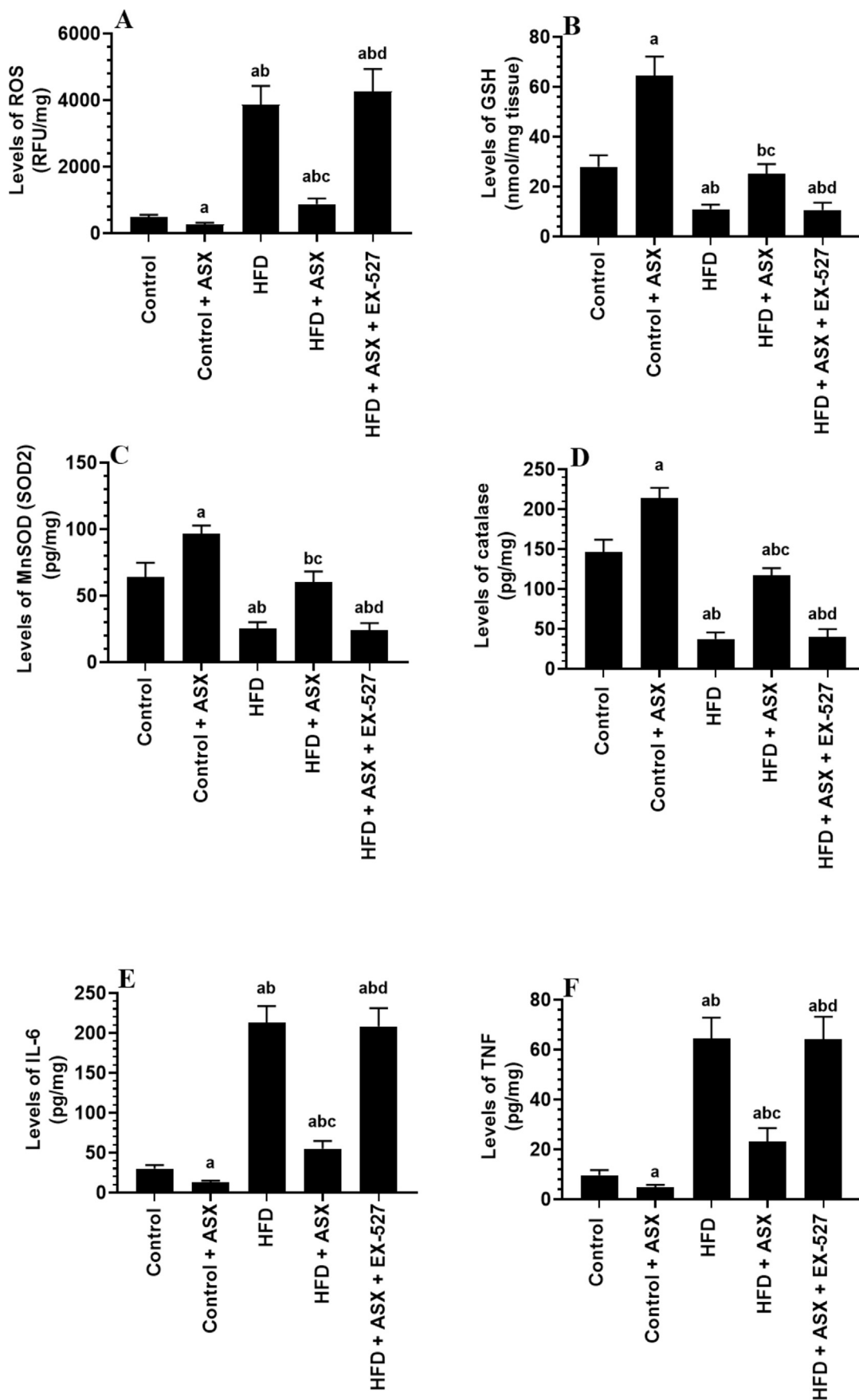


Fig. 3. Levels of ROS (A), GSH (B), MnSOD (C), catalase (D), IL-6 (E), and TNF- α (F) in the left ventricles (LVs) of all groups of rats. Data were analyzed for n = 10 samples/group and were significantly different $p < 0.05$. ^a: vs. the control rats; ^b: vs. the control + ASX-treated rats; ^c: vs. HFD-fed rats, ^d: vs. HFD + ASX-treated rats. EX-527: a selective SIRT1 inhibitor.

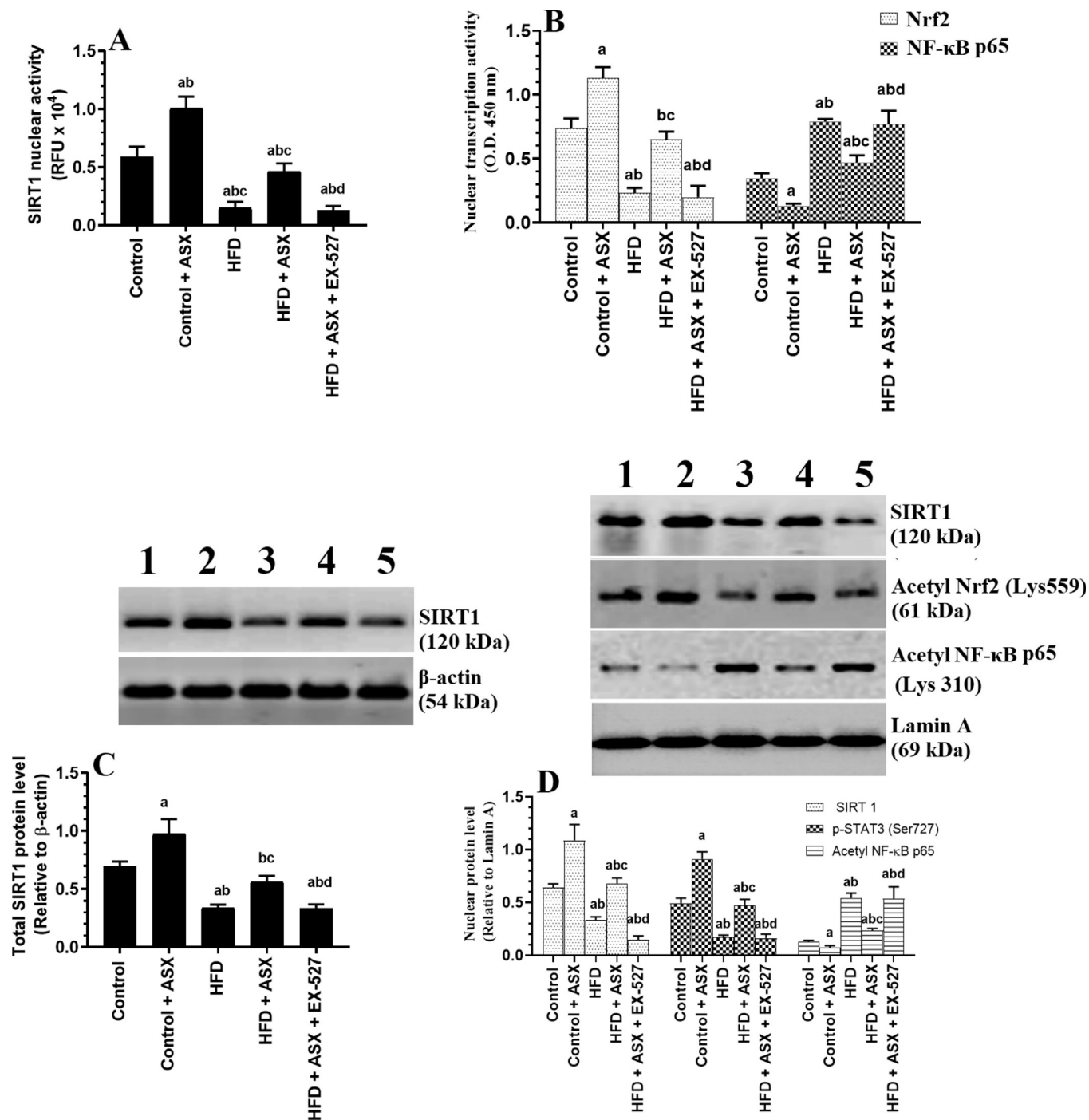


Fig. 4. Nuclear activity of SIRT1 (A), the nuclear activity of Nrf2 and NF-κB p65 (B), total protein levels of SIRT1 (C), and nuclear protein levels of SIRT1, acetyl Nrf2, and acetyl NF-κB p65 in the left ventricles (LVs) of all groups of rats. Data were analyzed for n = 6 samples/group and were significantly different $p < 0.05$. ^a: vs. the control rats; ^b: vs. the control + ASX-treated rats; ^c: vs. HFD-fed rats; ^d: vs. HFD + ASX-treated rats. EX-527: a selective SIRT1 inhibitor.

microembolization-induced cardiomyocyte apoptosis by upregulating Nrf2 (Xue et al., 2019).

Nevertheless, SIRT1 levels are significantly depleted in the hearts of obese and diabetic animals and are considered a major mechanism for the accelerated cardiac damage and remodeling in these animal models. As a cellular protective molecule, SIRT1 can deacetylate and activate Nrf2 and FOXO1/3a to stimulate the intracellular antioxidant gene expression (Cheng et al., 2003). Besides, SIRT1 can inhibit NF-κB by deacetylating the p65 subunit (Cheng et al., 2003). Also, SIRT1 inhibits fibrosis by downregulating

the expression of TGF-β1 and TGF-β1 receptor type1 (TGF-βR1), reducing the phosphorylation and nuclear localization of p-Smad2/3, and deacetylation of Smad3 (Huang et al., 2014; Liu et al., 2019; Wang et al., 2018; Zeng et al., 2017). In the same with the above-mentioned studies, a similar reduction in the levels and activities of SIRT1 was also seen in the hearts of HFD-fed rats of this study. However, the most interesting finding in this study is that we are demonstrating that the protective effect of ASX against HFD-induced cardiomyopathy is mediated by activating SIRT1 signaling. Indeed, ASX stimulated SIRT1 levels and activities and con-

comitantly reduced the acetylation of Nrf2, NF- κ B p65, and Smad3, not only in the LVs of the HFD-fed rats but also in the LVs of the control rats. These data could explain the higher activities of Nrf2 and the reduction in the activities of NF- κ B p65 in the hearts of both groups of rats. To confirm our data, we have treated the HFD-fed rats with EX-527 in the presence of ASX. As expected, all the obvious cardioprotective effects, as well as the reduction in the acetylation of all studied transcription factors afforded by ASX, were prevented by EX-527. Based on these findings, we become very confident that ASX could alleviate HFD-induced cardiac damage and remodeling by activating SIRT1 signaling. These findings support those reported by Zhang et al. (Zhang et al., 2017) who have shown that ASX alleviates cardiac damage and fibrosis in the LVs of rats with pressure overload-induced cardiomyopathy by upregulating and activating SIRT1 and subsequent increase in antioxidant levels and suppression of inflammatory cytokines production.

Despite these findings, this study still has some limitations. To confirm our results, further studies using SIRT1 knockdown animals or cardiomyocytes should be conducted. Besides, if other upstream mechanisms regulating SIRT1 are involved in the protective effect of ASX should be further investigated.

In conclusion, the present study have shown interesting findings and that a continuous administration of ASX has a protective effect to prevent HFD-induced cardiomyopathy in rats, at least by stimulating SIRT1. Given the well-reported highly tolerance and safety of ASX, further clinical studies using ASX as a therapy, at the levels of the heart or other disorders where SIRT1 is linked to the pathogenesis of the disorders, are encouraged to be conducted.

Declaration of Competing Interest

The authors declare that they have no known competing financial interests or personal relationships that could have appeared to influence the work reported in this paper.

Acknowledgment

The authors would like to thank the deanship of scientific research at King Khalid University for the continued support for this research and would like to thank their technical staff for their significant help to this study.

Funding

This study is funded by the deanship of scientific research at King Khalid University. Grant number (R.G.P.1/228/41)

References

Aimo, A., Castiglione, V., Borrelli, C., Saccaro, L.F., Franzini, M., Masi, S., Emdin, M., Giannoni, A., 2020. Oxidative stress and inflammation in the evolution of heart failure: From pathophysiology to therapeutic strategies. *Europ. J. Preventive Cardiol.* 27 (5), 494–510. <https://doi.org/10.1177/2047487319870344>.

Adluri, R.S., Thirunavukkarasu, M., Zhan, L., Maulik, N., Svennevig, K., Bagchi, M., Maulik, G., 2013. Cardioprotective efficacy of a novel antioxidant mix VitaPro against ex vivo myocardial ischemia-reperfusion injury. *Cell Biochem. Biophys.* 67, 281–286.

Aoi, W., Naito, Y., Sakuma, K., Kuchide, M., Tokuda, H., Maoka, T., Toyokuni, S., Oka, S., Yasuhara, M., Yoshikawa, T., 2003. Astaxanthin limits exercise-induced skeletal and cardiac muscle damage in mice. *Antioxid. Redox Signal.* 5 (1), 139–144.

Arunkumar, E., Bhuvanewari, S., Anuradha, C.V., 2012. An intervention study in obese mice with astaxanthin, a marine carotenoid—effects on insulin signaling and pro-inflammatory cytokines. *Food Funct.* 3 (2), 120–126.

Bhuvanewari, S., Anuradha, C.V., 2012. Astaxanthin prevents loss of insulin signaling and improves glucose metabolism in liver of insulin resistant mice. *Can. J. Physiol. Pharmacol.* 90 (11), 1544–1552.

Carbone, S., Canada, J.M., Billingsley, H.E., Siddiqui, M.S., Elagizi, A., Lavie, C.J., 2019. Obesity paradox in cardiovascular disease: where do we stand? *Vasc. Health Risk Manag.* 15, 89–100.

Cercato, C., Fonseca, F.A., 2019. Cardiovascular risk and obesity. *Diabetol. Metab. Syndr.* 11, 74.

Chan, K.C., Pen, P.J., Yin, M.C., 2012. Anticoagulatory and antiinflammatory effects of astaxanthin in diabetic rats. *J. Food Sci.* 77, H76–H80.

Choi, H.D., Kim, J.H., Chang, M.J., Kyu-Youn, Y., Shin, W.G., 2011. Effects of astaxanthin on oxidative stress in overweight and obese adults. *Phytother. Res.* 25 (12), 1813–1818.

Chong, Z.Z., Wang, S., Shang, Y.C., Maiese, K., 2012. Targeting cardiovascular disease with novel SIRT1 pathways. *Future Cardiol.* 8 (1), 89–100.

De Marchi, E., Baldassari, F., Bononi, A., Wieckowski, M.R., Pinton, P., 2013. Oxidative stress in cardiovascular diseases and obesity: role of p66Shc and protein kinase C. *Oxidative Med. Cell. Longevity.* article ID 564961.

Dludla, P.V., Joubert, E., Muller, C.J.F., Louw, J., Johnson, R., 2017. Hyperglycemia-induced oxidative stress and heart disease—cardioprotective effects of rooibos flavonoids and phenylpyruvic acid-2-O- β -D-glucoside. *Nutr. Metab. (Lond.)* 14, 45.

Dunlay, S. M., Givertz, M. M., Aguilar, D., Allen, L. A., Chan, M., Desai, A. S., Deswal, A., Dickson, V. V., Kosiborod, M. N., Lekavich, C. L., McCoy, R. G., Mentz, R. J., Piña, I. L., American Heart Association Heart Failure and Transplantation Committee of the Council on Clinical Cardiology; Council on Cardiovascular and Stroke Nursing; and the Heart Failure Society of America, 2019. Type 2 Diabetes Mellitus and Heart Failure: A Scientific Statement from the American Heart Association and the Heart Failure Society of America: This statement does not represent an update of the 2017 ACC/AHA/HFSA heart failure guideline update. *Circulation* 140(7), e294–e324.

Ebong, I.A., Goff, D.C., Rodriguez, C.J., Chen, H., Bertoni, A.G., 2014. Mechanisms of heart failure in obesity. *Obesity Res. Clin. Pract.* 8 (6), e540–e548.

Elibol, B., Kilic, U., 2018. High Levels of SIRT1 Expression as a Protective Mechanism Against Disease-Related Conditions. *Front. Endocrinol. (Lausanne)* 9, 614.

Fassett, R.G., Coombes, J.S., 2011. Astaxanthin: a potential therapeutic agent in cardiovascular disease. *Mar. Drugs* 9 (3), 447–465.

Fassett, R.G., Coombes, J.S., 2012. Astaxanthin in cardiovascular health and disease. *Molecules* 17 (2), 2030–2048.

Favero, G., Franco, C., Stacchiotti, A., Rodella, L.F., Rezzani, R., 2020. Sirtuin1 Role in the Melatonin Protective Effects Against Obesity-Related Heart Injury. *Front. Physiol.* 11, 103.

Fry, J.L., Al Sayah, L., Weisbrod, R.M., Van Roy, I., Weng, X., Cohen, R.A., Bachschmid, M.M., Seta, F., 2016. Vascular Smooth Muscle Sirtuin-1 Protects Against Diet-Induced Aortic Stiffness. *Hypertension* 68 (3), 775–784.

Geng, Z., Fan, W.Y., Zhou, B., Ye, C., Tong, Y., Zhou, Y.B., Xiong, X.Q., 2019. FNDC5 attenuates obesity-induced cardiac hypertrophy by inactivating JAK2/STAT3-associated inflammation and oxidative stress. *J. Transl. Med.* 17, 107.

Gross, G.J., Lockwood, S.F., 2004. Cardioprotection and myocardial salvage by a disodium disuccinate astaxanthin derivative (Cardax). *Life Sci.* 75 (2), 215–224.

Gross, G.J., Lockwood, S.F., 2005. Acute and chronic administration of disodium disuccinate astaxanthin (Cardax) produces marked cardioprotection in dog hearts. *Mol. Cell. Biochem.* 272, 221–227.

Gutiérrez-Cuevas, J., Sandoval-Rodríguez, A., Meza-Rios, A., Monroy-Ramírez, H.C., Galicia-Moreno, M., García-Bañuelos, J., Santos, A., Armendariz-Borunda, J., 2021. Molecular Mechanisms of Obesity-Linked Cardiac Dysfunction: An Update on Current Knowledge. *Cells* 10 (3), 629.

Huang, X.-Z., Wen, D., Zhang, M., Xie, Q., Ma, L., Guan, Y.i., Ren, Y., Chen, J., Hao, C.-M., 2014. Sirt1 activation ameliorates renal fibrosis by inhibiting the TGF- β /Smad3 pathway. *J. Cell. Biochem.* 115 (5), 996–1005.

Hussein, G., Nakagawa, T., Goto, H., Shimada, Y., Matsumoto, K., Sankawa, U., Watanabe, H., 2007. Astaxanthin ameliorates features of metabolic syndrome in SHR/NDmcr-cp. *Life Sci.* 80 (6), 522–529.

Jindal, A., Whaley-Connell, A., Brietzke, S., Sowers, J.R., 2013. Therapy of obese patients with cardiovascular disease. *Current Opinion Pharmacol.* 13 (2), 200–204. <https://doi.org/10.1016/j.coph.2012.12.006>.

Kato, T., Kasai, T., Sato, A., Ishiwata, S., Yatsu, S., Matsumoto, H., Shitara, J., Murata, A., Shimizu, M., Suda, S., Hiki, M., Naito, R., Daida, H., 2020. Effects of 3-Month Astaxanthin Supplementation on Cardiac Function in Heart Failure Patients with Left Ventricular Systolic Dysfunction—A Pilot Study. *Nutrients* 12.

Kavitha, K., Kowshik, J., Kishore, T.K.K., Baba, A.B., Nagini, S., 2013. Astaxanthin inhibits NF- κ B and Wnt/ β -catenin signaling pathways via inactivation of Erk/ MAPK and PI3K/Akt to induce intrinsic apoptosis in a hamster model of oral cancer. *Biochim. Biophys. Acta.* 1830 (10), 4433–4444.

Kim, S.H., Kim, H., 2018. Inhibitory Effect of Astaxanthin on Oxidative Stress-Induced Mitochondrial Dysfunction—A Mini-Review. *Nutrients* 10.

Landon, R., Gueguen, V., Petite, H., Letourneur, D., Pavon-Djavid, G., Anagnostou, F., 2020. Impact of Astaxanthin on Diabetes Pathogenesis and Chronic Complications. *Mar. Drugs* 18.

Liu, Q., Chen, Y.i., Auger-Messier, M., Molkentin, J.D., 2012. Interaction between NF κ B and NFAT coordinates cardiac hypertrophy and pathological remodeling. *Circ. Res.* 110 (8), 1077–1086.

Liu, Z.H., Zhang, Y., Wang, X., Fan, X.F., Zhang, Y., Li, X., Gong, Y.S., Han, L.P., 2019. SIRT1 activation attenuates cardiac fibrosis by endothelial-to-mesenchymal transition. *Biomed. Pharmacother.* 118, 109227.

Lockwood, S.F., Gross, G.J., 2005. Disodium disuccinate astaxanthin (Cardax): antioxidant and antiinflammatory cardioprotection. *Cardiovasc. Drug Rev.* 23, 199–216.

Matsushima, S., Sadoshima, J., 2015. The role of sirtuins in cardiac disease. *Am. J. Physiol. Heart Circ. Physiol.* 309 (9), H1375–H1389.

- Mohtavinejad, N., Nakhaee, A., Harati, H., Poodineh, J., Afzali, M., 2015. SIRT1 gene is associated with cardiovascular disease in the Iranian population. *Egypt. J. Med. Human Genet.* 16 (2), 117–122.
- Nakamura, M., Sadoshima, J., 2020. Cardiomyopathy in obesity, insulin resistance and diabetes. *J. Physiol.* 598 (14), 2977–2993.
- Nakao, R., Nelson, O.L., Park, J.S., Mathison, B.D., Thompson, P.A., Chew, B.P., 2010. Effect of astaxanthin supplementation on inflammation and cardiac function in BALB/c mice. *Anticancer Res.* 30, 2721–2725.
- Pan, X., Zhang, K., Shen, C., Wang, X., Wang, L., Huang, Y.Y., 2020. Astaxanthin promotes M2 macrophages and attenuates cardiac remodeling after myocardial infarction by suppression inflammation in rats. *Chin. Med. J. (Engl.)* 133, 1786–1797.
- Park, J.S., Chyun, J.H., Kim, Y.K., Line, L.L., Chew, B.P., 2010. Astaxanthin decreased oxidative stress and inflammation and enhanced immune response in humans. *Nutr. Metab. (Lond.)* 7, 18.
- Preuss, H.G., Echard, B., Yamashita, E., Perricone, N.V., 2011. High dose astaxanthin lowers blood pressure and increases insulin sensitivity in rats: are these effects interdependent? *Int. J. Med. Sci.* 8 (2), 126–138.
- Priyadarshini, L., Aggarwal, A., 2018. Astaxanthin inhibits cytokines production and inflammatory gene expression by suppressing I κ B kinase-dependent nuclear factor κ B activation in pre and postpartum Murrah buffaloes during different seasons. *Vet. World.* 11 (6), 782–788.
- Shatoor, A.S., Al Humayed, S., 2020. The Protective Effect of Crataegus aronia Against High-Fat Diet-Induced Vascular Inflammation in Rats Entails Inhibition of the NLRP-3 Inflammasome Pathway. *Cardiovasc. Toxicol.* 20 (1), 82–99.
- Shen, M., Chen, K., Lu, J., Cheng, P., Xu, L., Dai, W., Wang, F., He, L., Zhang, Y., Chengfen, W., Li, J., Yang, J., Zhu, R., Zhang, H., Zheng, Y., Zhou, Y., Guo, C., 2014. Protective effect of astaxanthin on liver fibrosis through modulation of TGF- β 1 expression and autophagy. *Mediators Inflamm.* 2014, 954502.
- Suthahar, N., Meijers, W.C., Siljé, H.H.W., de Boer, R.A., 2017. From Inflammation to Fibrosis-Molecular and Cellular Mechanisms of Myocardial Tissue Remodelling and Perspectives on Differential Treatment Opportunities. *Curr. Heart Fail. Rep.* 14 (4), 235–250.
- Tsutsui, H., Kinugawa, S., Matsushima, S., 2011. Oxidative stress and heart failure. *American journal of physiology. Heart Circulatory Physiol.* 301 (6), H2181–H2190.
- Wakabayashi, K., Hamada, C., Kanda, R., Nakano, T., Ito, H., Horikoshi, S., Tomino, Y., 2015. Oral Astaxanthin Supplementation Prevents Peritoneal Fibrosis in Rats. *Perit. Dial. Int.* 35 (5), 506–516.
- Wang, S., Wang, C., Turdi, S., Richmond, K.L., Zhang, Y., Ren, J., 2018. ALDH2 protects against high fat diet-induced obesity cardiomyopathy and defective autophagy: role of CaM kinase II, histone H3K9 methyltransferase SUV39H, Sirt1, and PGC-1 α deacetylation. *Int. J. Obes. (Lond.)* 42 (5), 1073–1087.
- Webber, M., Jackson, S.P., Moon, J.C., Captur, G., 2020. Myocardial Fibrosis in Heart Failure: Anti-Fibrotic Therapies and the Role of Cardiovascular Magnetic Resonance in Drug Trials. *Cardiol. Ther.* 9 (2), 363–376.
- Xue, Y., Sun, C., Hao, Q., Cheng, J., 2019. Astaxanthin ameliorates cardiomyocyte apoptosis after coronary microembolization by inhibiting oxidative stress via Nrf2/HO-1 pathway in rats. *Naunyn. Schmiedebergs Arch. Pharmacol.* 392 (3), 341–348.
- Zeng, Z., Cheng, S., Chen, H., Li, Q., Hu, Y., Wang, Q., Zhu, X., Wang, J., 2017. Activation and overexpression of Sirt1 attenuates lung fibrosis via P300. *Biochem. Biophys. Res. Commun.* 486, 1021–1026.
- Zhang, J., Xu, P., Wang, Y., Wang, M., Li, H., Lin, S., Mao, C., Wang, B., Song, X., Lv, C., 2015. Astaxanthin prevents pulmonary fibrosis by promoting myofibroblast apoptosis dependent on Drp1-mediated mitochondrial fission. *J. Cell. Mol. Med.* 19 (9), 2215–2231.
- Zhang, Y., Connelly, K.A., Thai, K., Wu, X., Kapus, A., Kepecs, D., Gilbert, R.E., 2017. Sirtuin 1 Activation Reduces Transforming Growth Factor- β 1-Induced Fibrogenesis and Affords Organ Protection in a Model of Progressive, Experimental Kidney and Associated Cardiac Disease. *Am. J. Pathol.* 187 (1), 80–90.
- Zhu, X., Chen, Y., Chen, Q., Yang, H., Xie, X.i., 2018. Astaxanthin Promotes Nrf2/ARE Signaling to Alleviate Renal Fibronectin and Collagen IV Accumulation in Diabetic Rats. *J. Diabetes Res.* 2018, 1–7.